Infrared reflectance of optical phonon modes in AlGaN epitaxial layers grown on sapphire substrates

Jun-Rong Chen, Tien-Chang Lu*, Gen-Sheng Huang, Tsung-Shine Ko, Hao-Chung Kuo, Shing-Chung Wang

Department of Photonics and Institute of Electro-Optical Engineering, National Chiao Tung University, 1001 Ta Hsueh Rd., Hsinchu, 30010 Taiwan

ABSTRACT

We reported the systematical study of optical properties of hexagonal $Al_xGa_{1-x}N$ epitaxial films grown on *c*-sapphire substrate using metal-organic chemical vapor deposition. By performing Fourier transform infrared spectroscopy measurements, the high-frequency dielectric constants and phonon frequencies can be obtained by theoretically fitting the experimental infrared reflectance spectra using a four-phase layered model. The high-frequency dielectric constant of $Al_xGa_{1-x}N$ varies between 4.98 and 4.52 for $\varepsilon_{\infty,\perp}$ (polarization perpendicular to the optical axis) and between 4.95 and 4.50 for $\varepsilon_{\infty,//}$ (polarization parallel to the optical axis) respectively when the aluminum composition changes from 0.15 to 0.24. Furthermore, from experimental infrared reflectance spectra of $Al_xGa_{1-x}N$ films, a specific absorption dip at 785 cm^{-1} was observed when the aluminum composition is larger than 0.24. The dip intensity increases and the dip frequency shifts from 785 to 812 cm^{-1} as aluminum composition increases from 0.24 to 0.58. According to the reciprocal space map of x-ray diffraction measurements, the emergence of this dip could be resulted from the effects of strain relaxation in AlGaN epitaxial layers due to the large lattice mismatch between GaN and AlGaN epitaxial film.

Keywords: AlGaN, Sapphire, Infrared reflectance, FTIR

1. INTRODUCTION

Hexagonal GaN and AlN semiconductors, and AlGaN alloys, have attracted considerable attention due to their successful applications in the fabrication of high-performance electronic and optoelectronic devices, such as heterostructure field-effect transistors,[1] ultra-violet light-emitting diodes,[2] and laser diodes.[3-5] By varying the alloy composition, different electrical and optical properties can be obtained in a wide spectral range from 3.4 to 6.3 eV. In order to further engineer these alloys and related optoelectronic devices, it is necessary to work on the fundamental properties of these materials. The infrared optical response of these alloys is important for the determination of crystal quality and phonon properties. Recently, Sun *et al*. proposed the idea of developing terahertz quantum cascade lasers with GaN/AlGaN quantum-well structures, which have more advantages than GaAs-based material system.[6] Since the carrier dynamics and temperature-dependent performance of quantum cascade lasers are closely related to the phonon energies, the study of composition-dependent phonon energies will be also conducive to the design and develop of nitride-based quantum cascade lasers. Generally, GaN, AlN, and $Al_xGa_{1-x}N$ alloys can be deposited on sapphire, silicon carbide, silicon, or GaAs substrates by using different growth methods.[7, 8] Except for GaAs substrates, GaN and its related compounds grown on these substrates have the hexagonal wurtzite structure (α-phase). Therefore, they are natural optically anisotropic uniaxial crystals.[9] In the hexagonal $Al_xGa_{1-x}N$ alloys with space group C_{6v}^4, both the transverse-optical (TO) and longitudinal-optical (LO) modes spit into the axial (A_1) and planar (E_1) optical modes due to the anisotropy in the macroscopic electric field induced by polar phonons. The A_1 and E_1 modes are both infrared and Raman active according to the selection rules. Yu *et al*. studied the infrared reflectivity spectra of GaN and $Al_xGa_{1-x}N$ with aluminum compositions of 0.087, 0.27, and 0.35.[10] They found that the E_2 mode, which arises from the disordered state of the alloys, can be observed in the refractivity spectrum of $Al_xGa_{1-x}N$. Holtz *et al*. reported optical studies on $Al_xGa_{1-x}N$ alloy layers grown on (111)-oriented silicon substrates by combining Fourier transform infrared (FTIR) and Raman spectroscopy studies.[11] Besides, Hu *et al*. studied the optical properties of hexagonal $Al_xGa_{1-x}N$ (x from 0.05 to 0.42) epitaxial films with Si doping concentration up to 10^{18} cm^{-3} grown on c-plane sapphire substrates using infrared

*timtclu@mail.nctu.edu.tw; phone +886-3-571-2121 ext. 31234; fax +886-3-571-6631

Gallium Nitride Materials and Devices III, edited by Hadis Morkoç, Cole W. Litton, Jen-Inn Chyi, Yasushi Nanishi, Euijoon Yoon, Proc. of SPIE Vol. 6894, 68941U, (2008) · 0277-786X/08/$18 · doi: 10.1117/12.760296

Downloaded From: http://proceedings.spiedigitallibrary.org/ on 04/25/2014 Terms of Use: http://spiedl.org/terms

reflectance spectra.[12] The longitudinal-optical phonon plasmon (LPP) coupled modes of *n*-type hexagonal $Al_xGa_{1-x}N$ films were also discussed in their studies. Nevertheless, the phonon-related studies on $Al_xGa_{1-x}N$ epitaxial films mostly focus on the composition-dependent infrared spectroscopy. To the best of our knowledge, the effects of strain relaxation of $Al_xGa_{1-x}N$ epitaxial films on infrared reflectance spectra are hardly reported in literature.

In this study, we will discuss the composition dependence of infrared optical phonon modes in $Al_xGa_{1-x}N$ epitaxial layers grown on *c*-plane sapphire substrates using Fourier transform infrared reflectance measurements. The effects of strain relaxation of $Al_xGa_{1-x}N$ epitaxial films on infrared reflectance spectra are investigated as well. Furthermore, the infrared reflectance spectra of GaN/sapphire and $Al_xGa_{1-x}N$/GaN/sapphire are theoretically fitted by using the factorized form of the dielectric function for the entire frequency region measured.

2. EXPERIMENT

Hexagonal $Al_xGa_{1-x}N$ epitaxial films in an entire aluminum composition range were grown on c-plane sapphire substrates by metal-organic chemical vapor deposition (MOCVD). AlGaN films were deposited using a low-pressure vertical reactor (EMCORE D75) with a fast rotational susceptor. Trimethylgallium (TMG) and trimethylaluminum (TMAl) were used as group III precursors and ammonia (NH_3) as group V precursor, respectively. Hydrogen and nitrogen purified by purifier were used as the carrier gas. The rotating speed was controlled to be 900 rpm during the growth of epitaxial layers. The group III and V precursors were separated in two manifolds and mixed before they entered the reactor. Prior to material growth, the sapphire substrate was annealed in H_2 ambient at 1100 °C for 5 min to remove any residual impurities on the sapphire surface. Figure 1 shows a schematic diagram of the AlGaN layer with a GaN buffer on the sapphire (0001) substrate. For all samples, a normal 30-nm-thick GaN nucleation layer was deposited at 500 °C. Before growing a 0.4-μm-thick $Al_xGa_{1-x}N$ film, a 2-μm-thick GaN buffer layer was grown on the GaN nucleation layer. All the growth conditions of GaN buffer layers were the same. $Al_xGa_{1-x}N$ epilayers in composition range of $0 < x < 0.3$ were grown in N_2 and H_2 mixture ambient gas and at pressure of 100 Torr. For the composition range of $0.3 < x < 1$, the $Al_xGa_{1-x}N$ epilayers were grown in N_2 and H_2 mixture ambient gas and at pressure of 50 Torr in order to obtain a better aluminum incorporation efficiency.[13] For the AlN epilayers, in order to obtain better crystal quality, the samples were grown in a pure N_2 ambient gas and at pressure of 100 Torr. The growth process was in-situ monitored by a filmetrics F-series thin-film measurement system.

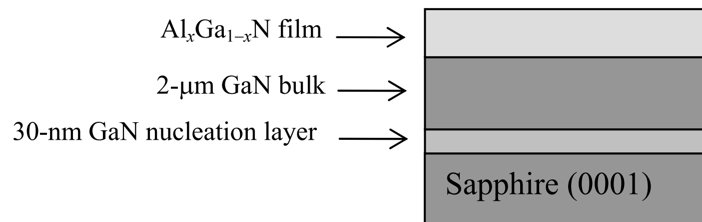

Fig. 1. Schematic diagram of the AlGaN thin film grown with GaN buffer layer on a sapphire (0001) substrate.

The compositions and crystal quality of $Al_xGa_{1-x}N$ films on GaN were measured by using a double crystal X-ray diffraction (Bede Scientific D1) and electron probe microanalyzer (JEOL JXA-8500F). The surface morphology was observed by atomic force microscope (AFM). The infrared reflectivity spectra were collected at room temperature by Bomen Fourier transform infrared spectrometer. We used nonpolarized light and a Fourier transform spectrometer, equipped with KBr beam splitter and a mercurcy-cadmium-tellride detector cooled down to 77 K. The incident angle with respect to the plane of incidence was kept at 75° (Brewster's angle was about 68°). The infrared reflectance spectrum of one-side-polished *c*-sapphire substrate was measured as well and no mathematical smoothing has been performed for the experimental reflectance spectra. The sample size should be lager than 1.5×1.5 cm^2 to collect the all reflected beams.

3. THEORY

Since hexagonal $Al_xGa_{1-x}N$ epilayers are uniaxial crystals, the *p* (electric-filed vector **E** parallel to the plane of incidence) and *s* (electric-field vector **E** perpendicular to the plane of incidence) modes of plane electromagnetic waves can not be

Downloaded From: http://proceedings.spiedigitallibrary.org/ on 04/25/2014 Terms of Use: http://spiedl.org/terms

independent of each other as the incident beam is oblique with optical axis, which is c-axis in hexagonal crystal system. Therefore, we employ a 4×4 matrix in order to calculate optical response of anisotropic media. This method is provided by Schubert and can be applied in the well-known transfer matrix method for multi-layer anisotropic meida.[14] The dielectric functions of anisotropic films in the x–y plane (perpendicular to the c axis, $\varepsilon_x = \varepsilon_y$) and in the z plane (parallel to the c axis) are $\varepsilon_\perp$ and $\varepsilon_{//}$, respectively. The total transfer matrix M_T can be expressed as the following product: $M_T = M_{in}M_1M_2M_{ex}$. Here, M_{in} and M_{ex} are the incident and exit matrices, respectively. The incident matrix M_{in} can be expressed as

$$M_{in} = \begin{bmatrix} 0 & 1 & -1/n_a\cos\Phi_a & 0 \\ 0 & 1 & 1/n_a\cos\Phi_a & 0 \\ 1/\cos\Phi_a & 0 & 0 & 1/n_a \\ -1/\cos\Phi_a & 0 & 0 & 1/n_a \end{bmatrix}. \quad (1)$$

The incident matrix M_{in} depends only on the angle of incidence Φ_a and the index of refraction n_a of the ambient material, which is unity for air in this study. M_1 and M_2 are the propagation matrix including the effects of crystal anisotropic properties and phase shift induced by layer thickness of the $Al_xGa_{1-x}N$ layer and GaN bulk underlying. The general form is expressed as

$$M = \begin{bmatrix} \cos(k_0 dN_{xz}) & 0 & 0 & i(N_{xz}/\varepsilon_x)\sin(k_0 dN_{xz}) \\ 0 & \cos(k_0 dN_{yy}) & -i(1/N_{yy})\sin(k_0 dN_{yy}) & 0 \\ 0 & -iN_{yy}\sin(k_0 dN_{yy}) & \cos(k_0 dN_{yy}) & 0 \\ i(\varepsilon_x/N_{xz})\sin(k_0 dN_{xz}) & 0 & n_x & \cos(k_0 dN_{xz}) \end{bmatrix}, \quad (2)$$

where d is the film thickness, $k_0 = 2\pi/\lambda$, λ is the incident wavelength, N_{xz} and N_{yy} can be obtained by applying Snell's law with the incident angle Φ_a,[15]

$$N_{xz} = \sqrt{\varepsilon_x}\sqrt{1-[(1/\sqrt{\varepsilon_z})\sin\Phi_a]^2}\ , \quad (3)$$

$$N_{yy} = \sqrt{\varepsilon_y}\sqrt{1-[(1/\sqrt{\varepsilon_y})\sin\Phi_a]^2}\ . \quad (4)$$

Furthermore, the exit matrix M_{ex} has following form

$$M_{ex} = \begin{bmatrix} 0 & 0 & \cos\Phi_z & 0 \\ 1 & 0 & 0 & 0 \\ -\sqrt{\varepsilon_{sy}}\cos\Phi_y & 0 & 0 & 0 \\ 0 & 0 & \sqrt{\varepsilon_{sx}} & 0 \end{bmatrix}, \quad (5)$$

where ε_{sx} and ε_{sy} are the anisotropic dielectric functions of sapphire substrates. The angle Φ_z and Φ_y can also be obtained applying Snell's law. The s and p-polarized reflectance can be written as follows:

$$R_s = \left|\frac{M_{10}M_{22} - M_{12}M_{20}}{M_{00}M_{22} - M_{02}M_{20}}\right|^2, \quad (6)$$

$$R_p = \left|\frac{M_{30}M_{02} - M_{32}M_{00}}{M_{20}M_{02} - M_{22}M_{00}}\right|^2. \quad (7)$$

It is noteworthy that the hexagonal nitride-based materials are uniaxial crystals. The s-polarized mode, whose electric-field vector **E** is perpendicular to the optics axis is known as the ordinary rays. Therefore, the s-polarized reflectance spectra have similar spectral shape under different angles of incidence. However, the p-polarized mode, whose electric-field vector **E** is perpendicular to the ordinary rays is the extraordinary rays. The p-polarized reflectance spectra are sensitive to the angles of incidence, which can effectively response the optical anisotropic properties.

Downloaded From: http://proceedings.spiedigitallibrary.org/ on 04/25/2014 Terms of Use: http://spiedl.org/terms

Since the reststrahlen regions of sapphire overlap with those of GaN and AlGaN, it is difficult to identify the phonon frequencies directly from the measured infrared reflectance spectra. Separately modeling the reflectance spectra of sapphire, GaN/sapphire, and AlGaN/GaN/sapphire is necessary to extract the phonon modes and dielectric function of each layer. A three-phase layered model is used to calculate the reflectance spectra of air/GaN/sapphire. We applied the obtained fitting parameters of the three-phase model in the subsequent four-phase model calculations for the $Al_xGa_{1-x}N$ epilayers (air/$Al_xGa_{1-x}N$/GaN/sapphire).[16] For uniaxial crystal, the dielectric tensor ε is required to completely describe the optical properties,[11, 17]

$$\varepsilon = \begin{bmatrix} \varepsilon_x & 0 & 0 \\ 0 & \varepsilon_y & 0 \\ 0 & 0 & \varepsilon_z \end{bmatrix} = \begin{bmatrix} \varepsilon_\perp & 0 & 0 \\ 0 & \varepsilon_\perp & 0 \\ 0 & 0 & \varepsilon_{//} \end{bmatrix} \quad (8)$$

For polar semiconductor materials, the contribution of l polar crystal lattice modes to the infrared dielectric function at photon energy $\hbar\omega$ can be expressed using a factorized model with Lorentzian broadening,[10, 18–20]

$$\varepsilon(\omega) = \varepsilon_{\infty,j} \prod_{i=1}^{l} \frac{\omega_{\mathrm{LO},ij}^2 - i\gamma_{\mathrm{LO},ij}\omega - \omega^2}{\omega_{\mathrm{TO},ij}^2 - i\gamma_{\mathrm{TO},ij}\omega - \omega^2}, \quad (9)$$

where j is equal to "//" or "⊥", which denotes the dielectric functions and phonon frequencies parallel or perpendicular to the optic c axis, respectively. $\omega_{\mathrm{LO},ij}$, $\gamma_{\mathrm{LO},ij}$, $\omega_{\mathrm{TO},ij}$, and $\gamma_{\mathrm{TO},ij}$ represent the phonon frequency and the broadening value of the ith LO and TO phonon, respectively. The parameters $\omega_{\mathrm{TO},\perp}$, $\omega_{\mathrm{TO},//}$, $\omega_{\mathrm{LO},\perp}$, and $\omega_{\mathrm{LO},\perp}$ are equal to the common used notations of the frequencies of the E_1(TO), A_1(TO), E_1(LO), and A_1(LO) modes, respectively. The model parameters $\varepsilon_{\infty,//}$ and $\varepsilon_{\infty,\perp}$ are the high-frequency dielectric constants for polarization parallel and perpendicular to the optical axis, respectively. The best-fit parameter values including high-frequency dielectric constants and phonon modes (ω_{TO} and ω_{LO}) in equation (9) can be obtained using a Levenberg-Marquardt algorithm.[21] This approach is an efficient nonlinear calculation method for many parameters fitting. The fitting is based on minimizing the following error function δ:

$$\delta^2 = \frac{1}{N} \sum_{i=1}^{N} \left| R_{i,\mathrm{exp}} - R_{i,\mathrm{cal}} \right|^2, \quad (10)$$

where N is the number of experimental data points, and $R_{i,\mathrm{exp}}$ and $R_{i,\mathrm{cal}}$ are the experimental and calculated values, respectively.

4. RESULTS AND DISCUSSION

In order to investigate the phonon frequencies of GaN and $Al_xGa_{1-x}N$ epilayers on sapphire substrates, it is necessary to obtain the knowledge of the dielectric function for sapphire substrate and identify the influences from sapphire phonon modes. The infrared dielectric anisotropy and phonon modes of sapphire are completely studied by Schubert *et al.* using infrared spectroscopic ellipsometry.[20] They determined the ordinary and extraordinary infrared complex dielectric functions as well as all infrared-active phonon modes of single crystal c-sapphire for wavelengths from 3 to 30 μm. In this study, we directly applied all physical parameters of c-sapphire including two high-frequency dielectric constants, four distinct infrared-active modes with dipole-moment oscillation perpendicular to the c axis, and two modes with dipole-moment oscillation parallel to the c axis from the reported values by Schubert *et al.*. These lattice vibrations are split into longitudinal and transversal optical modes due to coulomb interaction.[22] Figure 2 shows the experimental infrared reflectance spectrum (dotted line) and calculated reflectance spectrum (solid line) by employing the physical parameters of c-sapphire from Table 1.[20] It is found that the calculated infrared reflectance spectrum of c-sapphire is in good agreement with the experimental result. Since the sapphire substrates are commercial available and stable in crystal quality, we do not numerically fit the measured reflectance spectrum of sapphire in this study. Figures 3 and 4 show the optical function within the infrared spectral range for the ordinary (solid lines) and the extraordinary (dotted lines) optical functions. The spectral positions of the E_u ($\mathbf{E}\perp c$) and A_{2u} ($\mathbf{E}//c$) phonon modes are indicated by brackets within the upper part of the graphs. The dotted brackets denote the LO phonons, and the solid brackets denote the TO phonons. The n and k optical functions provide important information about infrared absorption peak and phonon energies of sapphire substrate, and are critical references for subsequent numerical fitting about GaN/sapphire and AlGaN/GaN/sapphire structures.

Downloaded From: http://proceedings.spiedigitallibrary.org/ on 04/25/2014 Terms of Use: http://spiedl.org/terms

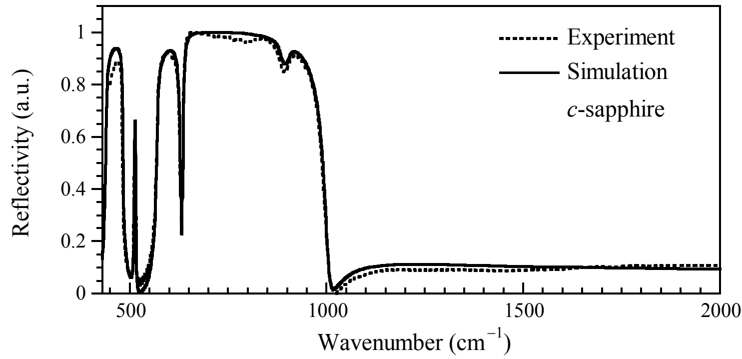

Fig. 2. Experimental (dotted line) and calculated (solid line) infrared reflectance spectra of the *c*-sapphire substrate.

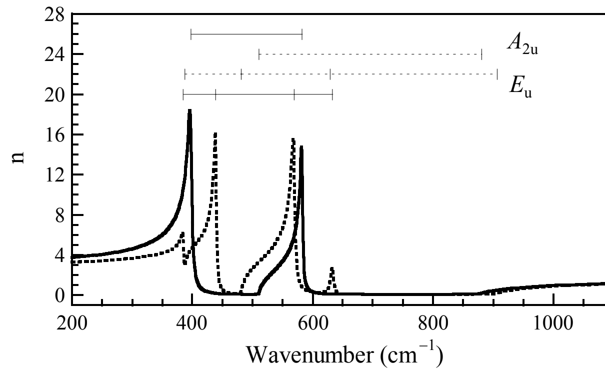

Fig. 3. Ordinary (solid line) and extraordinary (dotted line) refractive index for *c*-sapphire.

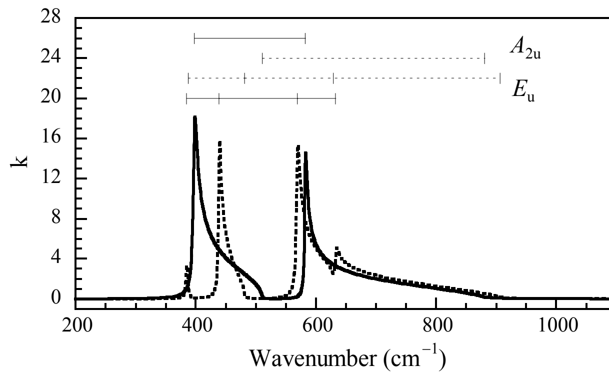

Fig. 4. Extinction coefficients of ordinary (solid line) ray and extraordinary (dotted line) ray for *c*-sapphire.

Table. 1. Physical parameters of *c*-sapphire used in the calculation.[20]

	ε_∞	ω_{TO} (cm^{-1})	ω_{LO} (cm^{-1})	γ_{TO}	γ_{LO}
E_u	3.077	384.99	387.60	3.3	3.1
		439.10	481.68	3.1	1.9
		569.00	629.50	4.7	5.9
		633.63	906.60	5.0	14.7
A_{2u}	3.072	397.52	510.87	5.3	1.1
		582.41	881.10	3.0	15.4

Downloaded From: http://proceedings.spiedigitallibrary.org/ on 04/25/2014 Terms of Use: http://spiedl.org/terms

The experimental (solid lines) and theoretical (dashed lines) infrared reflectance spectra of sapphire, GaN, AlN, and $Al_xGa_{1-x}N$ epitaxial films with aluminum composition x from 0.15 to 0.58 are shown in Fig. 5. It is obvious that there is a sharp dip at 755 cm^{-1} in GaN and all $Al_xGa_{1-x}N$ spectra compared with the spectra of sapphire. This dip is induced by LO phonon due to the optical anisotropy in the GaN material. Specifically, the *p*-polarized light of nonperpendicular incidence in the hexagonal epilayers can be interacted with the LO phonon mode and make it infrared active. For experimental reflectance spectra of $Al_xGa_{1-x}N$ films, the incorporation of 15% aluminum results in an additional dip at about 648 cm^{-1} as compared with that of GaN. Moreover, the dip intensity increases with the dip position slight shift of toward higher frequency when the aluminum composition increases in the range from 0.15 to 0.58. The dip was also observed in the experimental reflectance spectra of $Al_xGa_{1-x}N$ measured by Yu *et al.*.[10] They supposed the origin of this dip is related to the E_2 mode, which results from the random distribution of alloy constituents and the elimination of the translational symmetry of the lattice.

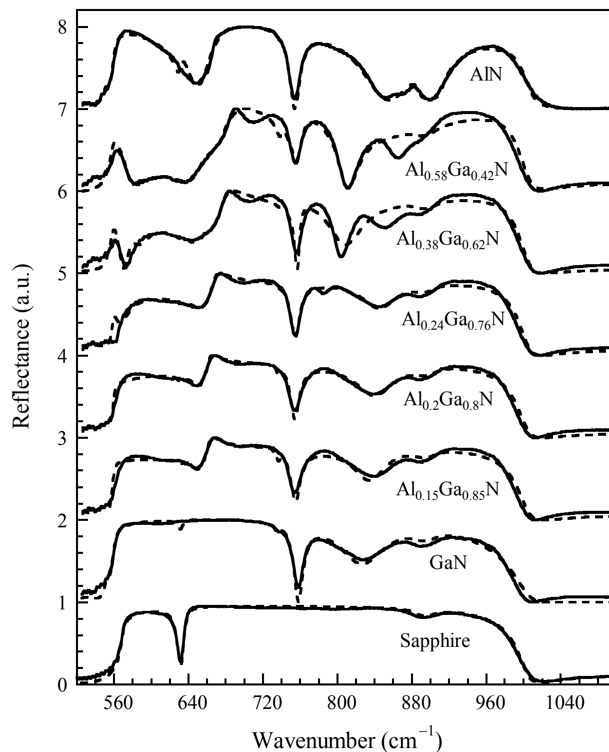

Fig. 5. Experimental (solid lines) and theoretical fitting (dashed lines) infrared reflectance spectra of sapphire, GaN on sapphire, and $Al_xGa_{1-x}N$ films on sapphire with different aluminum compositions.

In Fig. 5, it is found that when the aluminum composition is smaller than 0.24, the theoretical fitting reflectance spectra according to equation (9) are in good agreement with experimental results. However, when the aluminum composition is 0.24, a new dip at about 785 cm^{-1} can be observed in the experimental reflectance spectrum. The dip intensity increases with increasing aluminum composition and the dip frequency shifts from 785 to 812 cm^{-1} as aluminum composition increases from 0.24 to 0.58. In order to further investigate the origin of this dip, the reciprocal space maps (RSMs) of x-ray diffraction intensity of $Al_{0.2}Ga_{0.8}N$ and $Al_{0.24}Ga_{0.76}N$ films were performed around an asymmetrical GaN $(10\bar{1}5)$ Bragg peak as shown in Fig. 6. As depicted in Fig. 6 (a), the maximum of the $Al_{0.2}Ga_{0.8}N$ reciprocal lattice points is at fully strained position. Since the layer thicknesses of all $Al_xGa_{1-x}N$ films are nearly the same, we assume that the lattice constant of $Al_xGa_{1-x}N$ films with aluminum composition smaller than 0.2 is fully coherent to that of GaN bulk. Furthermore, when the aluminum composition of $Al_xGa_{1-x}N$ films increases from 0.2 to 0.24, the maximum of the $Al_{0.24}Ga_{0.76}N$ reciprocal lattice points shifts from a fully strained to a partially relaxed position, as shown in Fig. 6 (b). The degree of strain relaxation shall progressively increase with increasing aluminum composition under the condition of similar AlGaN layer thickness due to the large lattice mismatch between GaN and AlN. By comparing Fig. 5 and Fig. 6, it is found that the emergence of the dip at 785 cm^{-1} and the strain relaxation of AlGaN film occur at the same aluminum

Downloaded From: http://proceedings.spiedigitallibrary.org/ on 04/25/2014 Terms of Use: http://spiedl.org/terms

composition. Moreover, the dip intensity increases with aluminum composition, which results in the increased degree of strain relaxation as well. Therefore, we deduce that the origin of this dip is attributed to the strain relaxation of $Al_xGa_{1-x}N$ films. Since the phonon properties are closely related to the lattice vibration, crystal structure, and alloy composition, it can be expected that the fully strained, partially relaxed, and fully relaxed AlGaN films shall eliminate the translational symmetry of the lattice, which influences the phonon properties and is characterized from the infrared reflectance spectra. It is reasonable that the measured infrared reflectance spectra of $Al_xGa_{1-x}N$ films with aluminum composition larger than 0.24 cannot be excellently fitted by the symmetric physical model. The effect of strain relaxation of $Al_xGa_{1-x}N$ films should be considered in the determination of phonon frequency since it is difficult to grow fully strained AlGaN film with high aluminum composition.

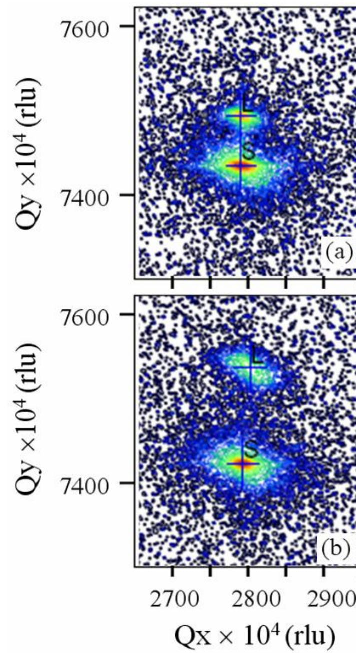

Fig. 6. Reciprocal space maps of (a) $Al_{0.2}Ga_{0.8}N$ and (b) $Al_{0.24}Ga_{0.76}N$ epitaxial films.

The best fitting parameters of GaN/sapphire, and $Al_xGa_{1-x}N$/GaN/sapphire with aluminum composition from 0.15 to 0.24 are shown in Table 2. Since the fitting parameters of the reflectance spectra of $Al_xGa_{1-x}N$ films with aluminum composition larger than 0.24 are not reliable due to the mismatch between measured and calculated reflectance spectra, these parameters are not shown in Table 2. The anisotropic high-frequency dielectric constants $\varepsilon_{\infty,\perp}$ and $\varepsilon_{\infty,//}$ decrease and the phonon frequency of ω_{TO} and ω_{LO} increase with increasing aluminum composition. The high-frequency dielectric constants of $Al_xGa_{1-x}N$ decrease from 4.98 to 4.52, which are located between the values of 5.01 for $Al_{0.087}Ga_{0.913}N$ and 4.5 for $Al_{0.27}Ga_{0.73}N$.[10]

Table. 2. Best fitting parameters of GaN/sapphire as well as $Al_xGa_{1-x}N$/GaN/sapphire with aluminum composition from 0.15 to 0.24 determined by infrared reflectance spectra.

	GaN	$Al_{0.15}Ga_{0.85}N$	$Al_{0.2}Ga_{0.8}N$	$Al_{0.24}Ga_{0.76}N$
$\varepsilon_{\infty,\perp}$	5.11	4.98	4.77	4.52
$\varepsilon_{\infty,//}$	5.07	4.95	4.65	4.50
$\omega_{TO,\perp}$ (cm^{-1})	559.1	565.2	570.3	575.8
$\omega_{TO,//}$ (cm^{-1})	533.1	542.1	545.3	550.7
$\omega_{LO,\perp}$ (cm^{-1})	742.2	775.1	787.6	790.2
$\omega_{LO,//}$ (cm^{-1})	734.5	762.1	775.8	780.6
$\omega_{TO,\perp}$ (cm^{-1})		628.6	625.9	623.7
$\omega_{TO,//}$ (cm^{-1})		638.3	640.2	643.7

Downloaded From: http://proceedings.spiedigitallibrary.org/ on 04/25/2014 Terms of Use: http://spiedl.org/terms

5. CONCLUSIONS

In summary, we have grown AlGaN films with different aluminum compositions for the study of composition-dependent phonon mode energies. The phonon mode frequency can be obtained from theoretically fitting the experimental FTIR spectra. However, we found that the calculated reflectivity spectra cannot be excellently fitted by the physical model when the aluminum composition is larger than 24%. According to asymmetrical RSMs measured around the GaN ($10\bar{1}5$) reflection, we suggest that this condition attributed to the emergence of a new dip at 785 cm^{-1} which can be observed as the strain relaxation of AlGaN film occurred. An advanced physical model is necessary for fitting the infrared reflectivity spectra of relaxed AlGaN films.

ACKNOWLEDGMENTS

This work is supported by the MOE ATU program and, in part, by the National Science Council of the Republic of China under Contract Nos. NSC 95-2120-M-009-008, NSC 95-2752-E-009-007-PAE, NSC 95-2221-E-009-282, and US Air Force Research Laboratory.

REFERENCES

1. N. Maeda, T. Saitoh, K. Tsubaki, T. Nishida, and N. Kobayashi, "Superior pinch-off characteristics at 400 °C in AlGaN/GaN heterostructure field effect transistors," Jpn. J. Appl. Phys. **38**, L987-L989 (1999).
2. T. Takano, Y. Narita, A. Horiuchi, and H. Kawanishi, "Room-temperature deep-ultraviolet lasing at 241.5 nm of AlGaN multiple-quantum-well laser," Appl. Phys. Lett., **84**, 3567-3569 (2004).
3. J. Han, M. H. Crawford, R. J. Shul, J. J. Figiel, M. Banas, L. Zhang, Y. K. Song, H. Zhou, and A. V. Nurmikko, "AlGaN/GaN quantum well ultraviolet light emitting diodes," Appl. Phys. Lett., **73**, 1688-1690, 1998.
4. V. Adivarahan, W. H. Sun, A. Chitnis, M. Shatalov, S. Wu, H. P. Maruska, and M. Asif Khan, "250 nm AlGaN light-emitting diodes," Appl. Phys. Lett., **85**, 2175-2177, 2004.
5. M. Shatalov, A. Chitnis, A. Koudymov, J. Zhang, V. Adivarahan, G. Simin, and M. A. Khan, "Differential carrier lifetime in AlGaN based multiple quantum well deep UV light emitting diodes at 325 nm," Jpn. J. Appl. Phys., **41**, L1146-L1148, 2002.
6. G. Sun, R. A. Soref, and J. B. Khurgin, "Active region design of a terahertz GaN/$Al_{0.15}Ga_{0.85}N$ quantum cascade laser," Superlattice. Microstruct., **37**, 107-113, 2005.
7. J. Li, J. Y. Lin, and H. X. Jiang, "Growth of III-nitride photonic structures on large area silicon substrates," *Appl. Phys. Lett.*, **88**, 171909-1-171909-3, 2006.
8. H. Morkoç, *Nitride Semiconductors and Devices*, Springer, Berlin, 1999.
9. S. Shokhovets, R. Goldhahn, G. Gobsch, S. Piekh, R. Lantier, A. Rizzi, V. Lebedev, and W. Richter, "Determination of the anisotropic dielectric function for wurtzite AlN and GaN by spectroscopic ellipsometry," J. Appl. Phys., **94**, 307-312, 2003.
10. G. Yu, H. Ishikawa, M. Umeno, T. Egawa, J. Watanabe, T. Soga, and T. Jimbo, "The infrared optical functions of $Al_xGa_{1-x}N$ determined by reflectance spectroscopy," Appl. Phys. Lett., **73**, 1472-1474, 1998.
11. M. Holtz, T. Prokofyeva, M. Seon, K. Copeland, J. Vanbuskirk, S. Williams, S. A. Nikishin, V. Tretyakov, and H. Temkin, "Composition dependence of the optical phonon energies in hexagonal $Al_xGa_{1-x}N$," J. Appl. Phys., **89**, 7977-7982, 2001.
12. Z. G. Hu, M. Strassburg, N. Dietz, A. G. U. Perera, A. Asghar and I. T. Ferguson, "Composition dependence of the infrared dielectric functions in Si-doped hexagonal $Al_xGa_{1-x}N$ films on *c*-plane sapphire substrates," Phys. Rev. B, **72**, 245326-1-245326-10, 2005.
13. G. S. Huang, H. H. Yao, T. C. Lu, H. C. Kuo, and S. C. Wang, "Aluminum incorporation into AlGaN grown by low-pressure metal organic vapor phase epitaxy," J. Appl. Phys., **99**, 104901-1-104901-5, 2006.
14. M. Schubert, "Polarization-dependent optical parameters of arbitrarily anisotropic homogeneous layered systems," Phys. Rev. B, **53**, 4265-4274, 1996.
15. R. M. A. Azzam and N. M. Bashara, *Ellipsometry and Polarized Light*, Amsterdam, North-Holland, 1997.
16. Z. G. Hu, M. Strassburg, A. Weerasekara, N. Dietz, A. G. U. Perera, M. H. Kane, A. Asghar, and I. T. Ferguson, "Lattice vibrations in hexagonal $Ga_{1-x}Mn_xN$ epitaxial films on *c*-plane sapphire substrates by infrared reflectance spectra," Appl. Phys. Lett., **88**, 061914-1-061914-3, 2006.

Downloaded From: http://proceedings.spiedigitallibrary.org/ on 04/25/2014 Terms of Use: http://spiedl.org/terms

[17] T. E. Tiwald, J. A. Woollam, S. Zollner, J. Christiansen, R. B. Gregory, T. Wetteroth, and S. R. Wilson, "Carrier concentration and lattice absorption in bulk and epitaxial silicon carbide determined using infrared ellipsometry," Phys. Rev. B, **60**, 11464-11474, 1999.
[18] D. W. Berreman and F. C. Unterwald, "Adjusting poles and zeros of dielectric dispersion to fit reststrahlen of $PrCl_3$ and $LaCl_3$," Phys. Rev., **174**, 791-799, 1968.
[19] A. Kasic, M. Schubert, S. Einfeldt, D. Hommel, and T. E. Tiwald, "Free-carrier and phonon properties of *n*- and *p*-type hexagonal GaN films measured by infrared ellipsometry," Phys. Rev. B, **62**, 7365-7377, 2000.
[20] M. Schubert, T. E. Tiwald, and C. M. Herzinger, "Infrared dielectric anisotropy and phonon modes of sapphire," Phys. Rev. B, **61**, 8187-8201, 2000.
[21] W. H. Press, S. A. Teukolsky, W. T. Vetterling, and B. P. Flannery, *Numerical Recipes in C: The Art of Scientific Computing*, Cambridge, Cambridge University Press, MA, 1992.
[22] A. B. Barker, "Infrared lattice vibrations and dielectric dispersion in corundum," *Phys. Rev.*, **132**, 1474-1481, 1963.

Downloaded From: http://proceedings.spiedigitallibrary.org/ on 04/25/2014 Terms of Use: http://spiedl.org/terms